

Momentum-space second-order optical potential for pion-nucleus elastic scattering

M. Gmitro

*Institute of Nuclear Physics, Czechoslovak Academy of Sciences, CS 250 68 Řež, Czechoslovakia
and Laboratory of Theoretical Physics, Joint Institute for Nuclear Research, Dubna, SU 101000 Moscow, U.S.S.R.*

S. S. Kamalov

Laboratory of Theoretical Physics, Joint Institute for Nuclear Research, Dubna, SU 101000 Moscow, U.S.S.R.

R. Mach

Institute of Nuclear Physics, Czechoslovak Academy of Sciences, CS 250 68 Řež, Czechoslovakia

(Received 12 January 1987)

For use in applications such as pion photoproduction and inelastic exclusive pion scattering studies, a first-plus-second-order pion-nucleus optical potential is constructed by fitting the phenomenological ρ^2 -dependent term to the π^\pm - ^{12}C total and differential cross sections. It is demonstrated that such a potential is A universal (A is the atomic mass number) and well describes all available (total and elastic differential) pion scattering data for the ^4He , ^6Li , ^{16}O , ^{28}Si , and ^{40}Ca targets in a broad energy range $14 \leq T_\pi \leq 250$ MeV.

I. INTRODUCTION

Presently, the theoretical models used to describe simultaneously the pion-nucleus scattering data at low ($T_\pi < 80$ MeV) and Δ -resonance energies are inspired by the Δ -hole excitation idea^{1,2} or by the multiple-scattering expansions.³⁻⁷ In both cases a truly microscopic approach has not yet been achieved since the pion interaction with two- (and possibly also more than two) nucleon clusters is treated only on the phenomenological level. That is, this important part of the interaction mechanism is only revealed by fitting both in the Δ -hole work ("spreading potential"; see e.g., Hirata *et al.*²) and, e.g., by Liu and Shakin⁶ in their optical model.

Our work is most similar in spirit to that of Ref. 6, where a microscopically constructed first-order pion-nucleus optical potential has been supplemented by a phenomenological second-order term which contains free parameters. The latter are energy dependent as indicated already in an earlier calculation,⁸ and in Ref. 6 they have been obtained by fitting the scattering data for the individual nuclei. Unfortunately, the parameters which came out from the fit⁶ change rather unsystematically both with the mass number A of the target nucleus and with the charge of the incoming pions even for the pion scattering by the isospin-zero nuclei. One can hardly believe that such features can consistently be explained in any microscopic calculation.

Here we would like to present another model of the pion-nucleus interaction inspired by the multiple-scattering theory. The model is rather simple and transparent in the parameter-free construction of the first-order optical potential. A nice feature is that the model then possesses a gratifying consistency: Being supplemented by a phenomenological term of the form $(B_0 + \mathbf{Q}' \cdot \mathbf{Q} C_0)G(|\mathbf{Q} - \mathbf{Q}'|)$, where $G(q)$ is the Fourier transform of the nuclear density squared, the model has

allowed us to find energy-dependent parameters $B_0(E)$ and $C_0(E)$ that are, however, universal with respect to the charge of pions and the atomic number of the target for nuclei up to $A = 40$.

Our expectation is that the present work can be useful not only as a practical tool of the data analysis of the inelastic processes [inelastic (π, π') scattering, (π, γ) photoproduction, etc.], but also as a guide for a further microscopic construction of the second-order optical potential. The numerical values of the parameters B_0 and C_0 as given in Table I and Fig. 1 are to be considered an extension—towards higher energies—of the threshold values extracted from the mesoatomic data, which are usually only discussed when microscopic models of the second-order terms are developed.^{8,9}

We shall work in the momentum representation. Such an approach affords definite technical merits; namely, it is computationally easier to control several features, such as the off-shell continuation of the πN amplitude, the transformation between π -nucleon and π -nucleus c.m. systems, the nucleon Fermi motion, and relativization of the equations. Similarly, the momentum-space methods are, by now, widely used also in the applications which we foresaw, e.g., in the pion photoproduction analysis.^{10,11}

In the construction of the first-order optical potential (Sec. II) we follow the multiple-scattering approach of Ref. 7. We do not introduce any free parameter at this level, with the possible exception of the off-shell parameter of the πN amplitude. After the first-order potential is constructed, we add to the potential the above-mentioned term proportional to the Fourier transform of the square of the nuclear density $\rho(r)$. At low energies of pions such a term is mainly due⁵ to the true pion absorption. Historically, Ericson, and Ericson¹² were probably the first who considered the ρ^2 term in the pion-nucleus optical potential. Landau and Thomas⁵ have considered the form $(B_0 + C_0 \mathbf{Q} \cdot \mathbf{Q}')G(q)$ and have taken the parameters B_0

and C_0 from the pion-deuteron absorption data. This has allowed them to improve considerably⁵ the description of the π - A scattering below 50 MeV. The parameters B_0 and C_0 adopted in Ref. 5 change by 20–33 % in the energy range 0–100 MeV. On the other hand, Chai and Riska⁸ foresee for them a strong energy dependence. We therefore consider B_0 and C_0 as free parameters and shall fix them in Sec. III from data on pion-¹²C scattering. The second-order potential thus obtained is then, in Sec. IV, applied to the low-energy and resonance energy scattering, taking ⁴He, ⁶Li, ¹⁶O, ²⁸Si, and ⁴⁰Ca as targets. The approximations adopted in the present work are summarized and discussed in Sec. V, and, finally, in Sec. VI, we give some conclusions on the results and significance of the present work.

II. FIRST-ORDER OPTICAL POTENTIAL IN THE MOMENTUM SPACE

We use a simple variant of the multiple scattering theories developed in detail in an earlier paper.⁷ Here we merely summarize the main features of the model.

Using the free-nucleon matrix $t(E)$ instead of the $\tau(E)$ appropriate for the bound nucleon (impulse approximation) and the nuclear optical potential $U(E)$ in the form $U(E) \approx At(E)$ (coherent scattering approximation), one has to solve the equation

$$T'(E) = U(E)[1 + G(E)\hat{P}T'(E)] \quad (1)$$

for the auxiliary matrix $T'(E)$, which is connected with the pion-nuclear matrix $T(E)$ as $T'(E) = (A - S)T(E)/A$. In Eq. (1), $G(E)$ is the pion-nucleus Green function and

the operator \hat{P} projects onto the nuclear ground state, $\hat{P} = |0\rangle\langle 0|$. The parameter S distinguishes between the Watson³ ($S=0$) and KMT (Ref. 4) ($S=1$) formulations of the multiple scattering theory.

The nucleon Fermi motion is treated here in the factorization approximation: Instead of averaging over the nucleonic motion, we use the effective values of the nucleon momenta (in the π -nucleus c.m. system)

$$\begin{aligned} \mathbf{p}_i \rightarrow \mathbf{p}_i^{\text{eff}} &= -\frac{\mathbf{Q}}{A} + \frac{A-1}{2A}(\mathbf{Q}' - \mathbf{Q}), \\ \mathbf{p}_f \rightarrow \mathbf{p}_f^{\text{eff}} &= -\frac{\mathbf{Q}'}{A} - \frac{A-1}{2A}(\mathbf{Q}' - \mathbf{Q}). \end{aligned} \quad (2)$$

Simultaneously, the π -nucleon matrix $t(E)$ is taken at an energy E , actually shifted by the amount

$$\Delta E = -\frac{\mu}{8\mathcal{M}} \frac{A-1}{A} (\mathbf{Q}' + \mathbf{Q})^2, \quad (3)$$

where \mathbf{Q} (\mathbf{Q}') is the pion momentum of the initial (final) state calculated in the π -nucleus c.m. system and the reduced mass of the pion-nucleon and pion-nucleus system is denoted by μ and \mathcal{M} , respectively.

The factorization approximation is indeed used for its simplicity. Still, the approximation is rather effective: In Ref. 13 it has been demonstrated that via factorization one actually takes into account a large portion of the medium corrections. This is probably due to the Galileo invariance of the potential resulting from our procedure (see Mach¹³), since then the effects left out are only of the order $(m_\pi/m_N)^2 \approx (\frac{1}{7})^2$.

Technically, for the pion-nucleus system we solve the equation

$$\langle \mathbf{Q}' | F(E) | \mathbf{Q} \rangle = \langle \mathbf{Q}' | V^{(1)}(z) | \mathbf{Q} \rangle - \frac{1}{2\pi^2} \int \frac{\langle \mathbf{Q}' | V^{(1)}(z) | \mathbf{Q}'' \rangle \langle \mathbf{Q}'' | F(E) | \mathbf{Q} \rangle}{Q^2 - Q''^2 + i\epsilon} d^3Q'', \quad (4)$$

where the first-order optical potential for the elastic scattering on the spin-zero, isospin-zero targets is

$$\begin{aligned} \langle \mathbf{Q}' | V^{(1)}(z) | \mathbf{Q} \rangle &= (A - S) \left[\frac{\mathcal{M}(Q')\mathcal{M}(Q)}{\mu(Q', k')\mu(Q, k)} \right]^{1/2} \\ &\times f_0(\mathbf{k}', \mathbf{k}, z) F_0(\mathbf{Q}' - \mathbf{Q}). \end{aligned} \quad (5)$$

Here, \mathbf{k} (\mathbf{k}') is the pion momentum in the πN c.m. system in the initial (final) state, f_0 is the scalar-isoscalar part of the πN scattering amplitude, and $F_0(\mathbf{Q}' - \mathbf{Q})$ is the Fourier transform of the appropriate nuclear density distribution. A separable form of the pion-nucleon amplitude was used in each partial wave (l, α) , where l stands for orbital momentum and α for spin and isospin quantum numbers. The pion-nucleon form factors

$$v_{l\alpha}(p) = p^l v(p), \quad v(p) = [1 + (r_0 p)^2]^{-2} \quad (6)$$

characterize the off-energy-shell behavior of the amplitude. When the choice $r_0 = 0.47$ fm was made, our $v_{l\alpha}(p)$ is very much like the πN separable potential⁵⁵ in the

resonating partial wave $l=1$ $\alpha = (\frac{3}{2}, \frac{3}{2})$.

The amplitude $F(E)$ obtained from Eq. (4) is connected with the needed $T(E)$ matrix via the relativistic expression

$$\langle \mathbf{Q}' | F(E) | \mathbf{Q} \rangle = -\frac{1}{2\pi} [\mathcal{M}(Q')\mathcal{M}(Q)]^{1/2} \langle \mathbf{Q}' | T(E) | \mathbf{Q} \rangle. \quad (7)$$

For the details of calculations we refer once again to Ref. 7. There, also, one finds the extension of Eq. (5) necessary for the spin-nonzero nuclei like ⁶Li considered in the present paper. Let us only note that Eq. (4) has been solved via the matrix inversion method,¹⁴ and the Coulomb interaction effects are treated as suggested by Vincent and Phatak.¹⁵

III. PARAMETRIZATION OF THE SECOND-ORDER POTENTIAL

Exploration^{7,16,17} of the above-described first-order optical model has shown that one obtains in this way a fair but unquantitative description of the data for the scatter-

ing of pions on the light nuclei. Definite disagreement (cf. dashed lines in Figs. 2–8) is observed between experimental and first-order theoretical results both at low and resonance energies. Clearly, a new dynamical input is needed to understand these features. It has been repeatedly suggested recently^{5,6} that such an input may have a form of a ρ^2 -dependent term. Physically, such a term may receive contributions from several processes. We mention here the true pion absorption (two-body or “deuteron-like” mechanism) and the processes left out when the impulse and coherent approximations have been adopted. Actually, for the last two corrections, Eisenberg and Koltun¹⁸ have derived an approximate form

$$f_0^2(z) A(A-1)G(\mathbf{Q}-\mathbf{Q}')R_{\text{correl}} .$$

where R_{correl} is the two-body correlation length. The contribution of such a term should be strongly energy dependent due to the resonance character of the pion-nucleon amplitude $f_0(z)$.

Taking together the above-mentioned suggestion of Landau and Thomas⁵ and the just discussed approximation by Eisenberg and Koltun,¹⁸ and in the absence of any trustworthy derivation of the second-order potential, we opted for a semiphenomenological approach, taking

$$\begin{aligned} \langle \mathbf{Q}' | V^{(2)}(E) | \mathbf{Q} \rangle &= (A-S)(A-1) \left[\frac{\mathcal{M}(\mathbf{Q}')\mathcal{M}(\mathbf{Q})}{m_\pi} \right]^{1/2} \\ &\times d \left[B_0(E) + C_0(E) \frac{\mathbf{Q}' \cdot \mathbf{Q}}{d^2} \right] \\ &\times \frac{v(\mathbf{Q}')v(\mathbf{Q})}{v^2(Q_0)} G(\mathbf{Q}'-\mathbf{Q}) , \end{aligned} \quad (8)$$

$$G(q) = \frac{4\pi}{q} \int r \rho^2(r) \sin qr \, dr ,$$

with the energy-dependent complex coefficients $B_0(E)$ and $C_0(E)$ to be determined from the data. The meaning of $v(Q)$ is the same as in Eq. (6). The kinematical factor $d = 1 + m_\pi/2m_N$, where $m_N(m_\pi)$ is the nucleon (pion) mass, has been introduced so that the parameters B_0 and C_0 in the low-energy limit coincide with the definitions usual in the mesoatomic studies.¹⁹ Actually, a very similar form of the second-order potential has been adopted by Liu and Shakin,⁶ the only differences being rather arbitrary kinematic factors and the shift in energy E at which the coefficients $B_0(E)$ and $C_0(E)$ are taken in the actual calculations. Assuming the dominance of two-nucleon processes in the second-order optical potential and having in mind the approximation of “independent nucleon pairs” (see. Ref. 20), the energy E is shifted by the amount

$$\Delta E = -\frac{\mu_2}{16M} \frac{A-2}{A} (\mathbf{Q}'+\mathbf{Q})^2 \rightarrow -\frac{\mu_2}{4M} \frac{A-2}{A} Q^2 , \quad (9)$$

where μ_2 is the reduced mass of the π -2N system, and the simplified expression on the extreme right of Eq. (9) has been used in the numerical work.

The term $-\Delta E$ stands for the energy of the center-of-mass motion of the π -2N system, provided the effective

values are used for the momenta of the 2N system,

$$\begin{aligned} \mathbf{p}_{2f}^{\text{eff}} &= -\frac{2\mathbf{Q}}{A} + \frac{A-2}{2A} (\mathbf{Q}'-\mathbf{Q}) , \\ \mathbf{p}_{2f}^{\text{eff}} &= -\frac{2\mathbf{Q}'}{A} - \frac{A-2}{2A} (\mathbf{Q}'-\mathbf{Q}) . \end{aligned} \quad (10)$$

The procedure adopted here is completely analogous to the factorization approximation which leads to Eqs. (2) and (3) in the case of the first-order optical potential. The only difference is that the kinematics of the π -N system is now replaced by that of the π -2N system.

As for the nuclear dynamics, it is fully contained in the nuclear density distribution $\rho(r)$ which enters into both Eqs. (5) and (8). It is clear that $G(q)$ of Eq. (8) is more sensitive to the details of $\rho(r)$ than the form factor $F(q)$ entering into Eq. (5). It is important, therefore, to use in the calculations an expression for $\rho(r)$ as realistic as possible. We have chosen for $\rho(r)$ the model of symmetrized Fermi density²¹ which correctly describes the nuclear electromagnetic form factors up to large momentum transfers. Our density $\rho_{\text{SF}}(r)$ corresponds, by construction,²¹ to the distribution of the nucleons with respect to the nucleus center of mass. The experimentally observed form factor is $F_{\text{expt}}(q) = f_N(q)F_{\text{SF}}(q)$, where F_{SF} is the Fourier transform of $\rho_{\text{SF}}(r)$ and $f_N(q) = (1+q^2/0.71 \text{ GeV}^2)^{-2}$ stands for the nucleon form factor. Further details concerning the calculations with the symmetrized Fermi density are given in the Appendix.

Investigation of pion single- and double-charge-exchange reactions on nuclei indicate strongly the presence of isovector and isotensor terms in the complete second-order optical potential. Such terms are not considered here and we refer the reader to the recent coordinate-space analyses⁵⁶ on this subject.

A. π -¹²C scattering

To establish the form of the energy dependence of B_0 and C_0 , we have used all available data on the elastic differential ($d\sigma/d\Omega$) and total (σ_T) cross sections for the π^+ -¹²C and π^- -¹²C scattering at energies $T_\pi \leq 250$ MeV. On the low-energy side we have paid attention to get the fitted results close enough to the values $B_0 = -0.043 + i0.043$ and $C_0 = -0.10 + i0.10$ extracted from the mesoatomic data.¹⁹ This is indeed only a very weak reference point, since these last values of B_0 and C_0 have been obtained using an optical potential¹⁹ very different from ours. Fortunately, as we shall see below, the $d\sigma/d\Omega$ at $T_\pi = 14$ and 20 MeV are not very sensitive to the small changes of B_0 and C_0 . The results of the best fit for B_0 and C_0 are given in Table I and Fig. 1.

In Fig. 2 we show the differential cross sections of the π^\pm -¹²C elastic scattering calculated with the first-order (dashed line) and first- plus second-order (solid line) potentials described above and compare them with data. The corresponding total and integral elastic cross sections are shown in Fig. 3.

Before discussing the form of the energy dependence obtained for the coefficients $B_0(E)$ and $C_0(E)$, we wish to comment shortly on the results for $d\sigma/d\Omega$ shown in Fig. 2.

TABLE I. Numerical values of the parameters B_0 (in units of m_π^{-4}) and C_0 (in units of m_π^{-6}) as obtained from fitting the differential cross sections and total cross sections of the π^\pm - ^{12}C scattering.

T_π	$\text{Re}B_0$	$\text{Im}B_0$	$\text{Re}C_0$	$\text{Im}C_0$
14	-0.05	0.05	-0.14	0.12
20	-0.05	0.04	-0.14	0.10
30	-0.05	0.025	-0.14	0.05
40	-0.05	0.01	-0.145	0.02
50	-0.05	0.005	-0.15	0
67.5	-0.045	0	-0.16	0
80	-0.020	0	-0.185	0
100	-0.01	0	-0.20	0
120	0	0	-0.25	0
135	0.05	-0.01	-0.27	-0.03
150	0.15	-0.08	-0.30	-0.10
162	0.30	-0.10	-0.35	-0.15
180	0.50	-0.12	-0.35	-0.20
200	0.40	-0.06	-0.17	-0.20
215	0.25	-0.01	-0.075	-0.13
230	0.15	0.02	0	-0.07
240	0.07	0.04	0.025	-0.03
260	0.02	0.04	0.05	-0.01
280	0	0.03	-0.05	0

(i) In Fig. 2(a) we compare the results obtained with B_0 and C_0 from Table I with those (dashed-double-dotted line) calculated using the above quoted mesoatomic estimates of B_0 and C_0 . It is clear from this comparison that the last ones fail to reproduce the elastic scattering data above $T_\pi=20$ MeV.

(ii) The π^+ - ^{12}C differential cross sections as measured at $T_\pi=65$ MeV (Ref. 28) and $T_\pi=67.5$ MeV (Ref. 27) seem to be in mutual contradiction: only the latter result can be described by a smooth variation of the fitted parameters. To match the $T_\pi=65$ MeV data, one would need $\text{Re}B_0=-0.01$, a value very far from the values -0.05 and -0.045 appropriate at the energies $T_\pi=50$ and 67.5 MeV, respectively. Our choice will further be supported by the results obtained for the 68 MeV pion scattering off ^4He shown in Fig. 4 and discussed in Sec. IV.

(iii) The π^+ - ^{12}C data at $T_\pi=100$ MeV near the first minimum go substantially higher than our calculated result. We have preferred not to force the fit here at the price of abrupt changes of B_0 and C_0 at these energies. It is interesting to mention that Antonuk *et al.*²⁹ in their very detailed analysis of the 100 MeV π^+ -elastic scattering on ^{12}C within the Δ -hole model have met a completely analogous difficulty. The deep minimum as calculated both in our approach and in Ref. 29 at $\theta=120^\circ$ is intimately connected with the minimum of the nuclear form factor. Surprisingly, in the case of π^+ - ^{16}O scattering the data in the same energy region support the appearance of such a minimum, see Fig. 6. This brings in an additional difficulty, since one should look for a mechanism which may help filling in the minimum in the case of ^{12}C and, simultaneously, leave the ^{16}O calculation intact.

(iv) The large-angle scattering at higher energies ($T_\pi > 160$ MeV) is probably too delicate to be accurately

described in a model like ours, where e.g., the angle dependence of some auxiliary quantities has been disregarded; see Sec. V for a more detailed discussion. Still we wish to stress that the inaccuracies only appear for the scattering angles beyond the second minimum; again, precisely the same feature has been observed in the Δ -hole calculation by Horikawa *et al.*,² see Fig. 4 of Ref. 2 for the 160 MeV pion scattering off ^{12}C .

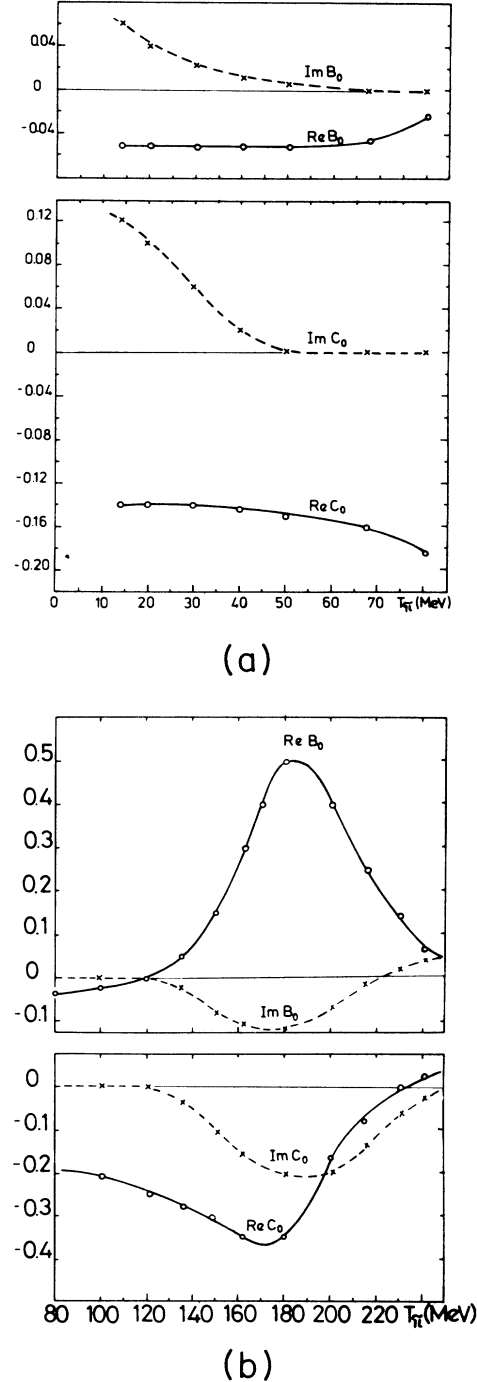


FIG. 1. Parameters B_0 in units of m_π^{-4} and C_0 in units of m_π^{-6} as functions of the pion kinetic energy.

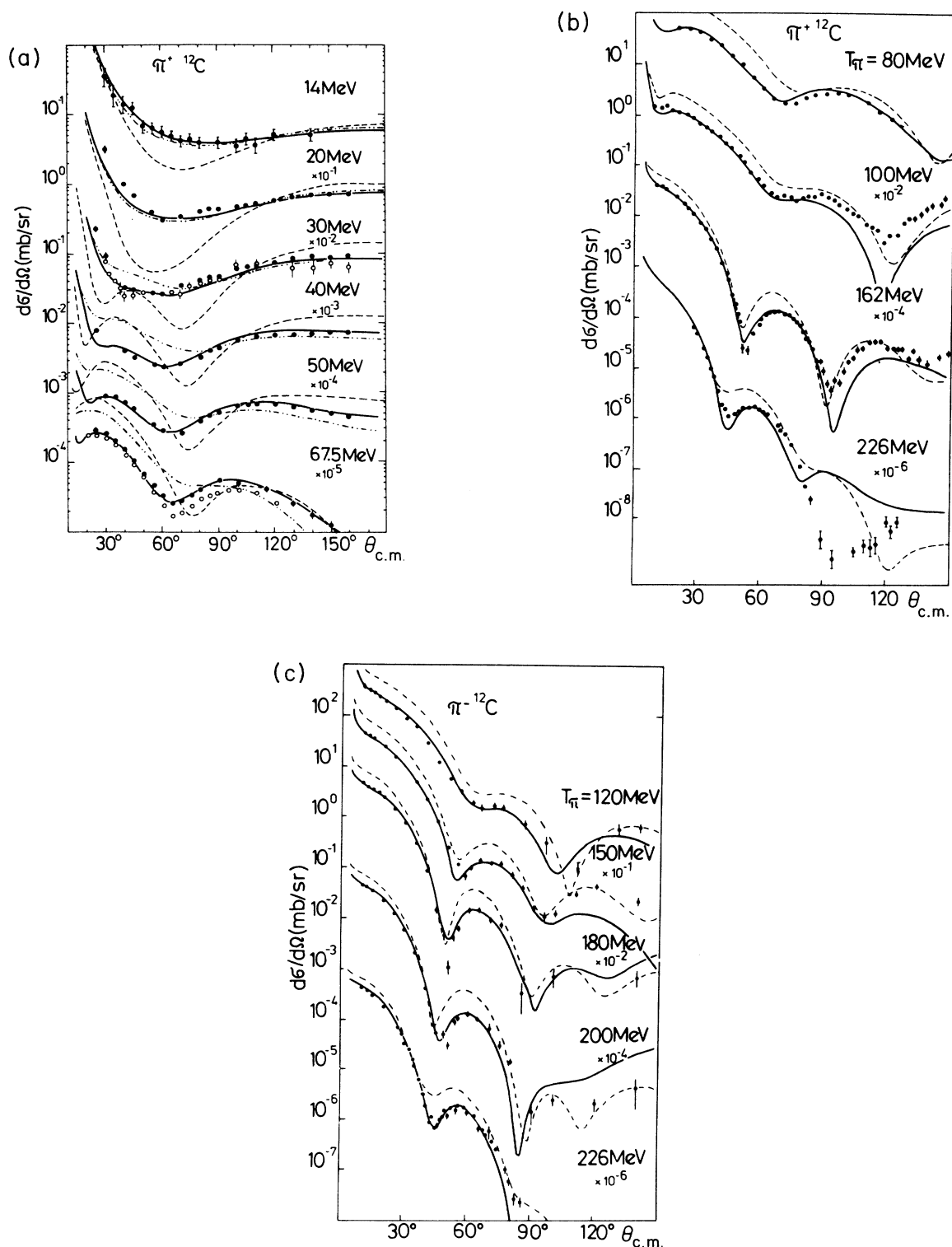


FIG. 2. Comparison of theoretical calculations with the data for π scattering from ^{12}C . The dashed curves represent the results for $V^{(1)}$ and the solid curves include the effects of $V^{(2)}$ with B_0 and C_0 taken from Table I, while the dashed-double-dotted line is obtained with $V^{(2)}$ calculated for mesoatomic values (Ref. 19) $B_0 = -0.043(1-i)$ and $C_0 = -0.10(1-i)$. Data are from the following references: (a) $T_\pi = 14$ MeV (Ref. 22), 20 MeV (Ref. 23), 30 MeV (Ref. 24; Ref. 26), 40 MeV (Ref. 25), 50 MeV (Ref. 24), 65 MeV (Ref. 28), 67.5 MeV (Ref. 27); (b) $T_\pi = 80$ MeV (Ref. 28), 100 MeV (Ref. 29), 162 and 226 MeV (Ref. 30); (c) $120 \leq T_\pi \leq 200$ MeV (Ref. 31), 226 MeV (Ref. 30; Ref. 31).

B. Energy dependence of the parameters B_0 and C_0

To start the discussion of the results obtained for B_0 and C_0 , it is worth stressing that both positive- and negative-charge pion scattering on ^{12}C have been described by a unique set of B_0 and C_0 .

An inspection of Fig. 1 reveals that both $\text{Im}B_0$ and $\text{Im}C_0$ decreases rapidly with increasing reaction energy ($15 \leq T_\pi \leq 50$ MeV) and are nearly zero in a broad interval between 50 and 120 MeV. Then, a deep valley appears with a minimum near the Δ -resonance energy. The behavior of our $\text{Im}B_0$ and $\text{Im}C_0$ near the resonance energy and those of Ref. 6 are rather similar. For the argument below it is important that the two phenomenological analyses arrived at large *negative* values of $\text{Im}B_0$ and $\text{Im}C_0$ around the resonance.

The interesting part is indeed the comparison with the earlier microscopic calculation of the parameters B_0 and C_0 in the resonance region, which has been attempted in Ref. 8. There, the authors assume that B_0 and C_0 receive their dominant contributions from the two-body absorption processes mediated by the exchange of π and ρ mesons. The calculation was performed within the Fermi-gas model and for infinite nuclear matter. In Ref. 8, $\text{Im}B_0$, $\text{Re}C_0$, and $\text{Im}C_0$ are all positive and a clear maximum of both $\text{Re}C_0$ and $\text{Im}C_0$ has been obtained near $T_\pi = 170$ MeV.

To understand the signs of the calculated⁸ and fitted (in Ref. 6 and the present results) values of $\text{Im}B_0$ and $\text{Im}C_0$, one should consider an intrinsic feature of the first-order optical potentials: Tandy, Redish, and Bollé³⁹ have shown that the imaginary part of the first-order optical potential is mainly responsible for the escape of the pions from the elastic to the quasielastic channel. Further, once the impulse approximation is used in evaluating the optical potential, the quasielastic contribution is treated only in the plane-wave approximation. According to general belief, the role of the quasielastic channel is then grossly overestimated. Our fitted values obtained for $\text{Im}B_0$ and $\text{Im}C_0$ (and indeed those of Liu and Shakin⁶ as well) seem to confirm such an interpretation of the imaginary part of the first-order optical potential: they are negative since $\text{Im}B_0 + Q \cdot Q' \text{Im}C_0$, first of all, should compensate for—especially in the resonance region—the overestimated (by the first-order potential) contribution to the total cross section of the quasielastic channel, rather than reflect the true absorption processes alone. On the other hand, the latter should apparently be considered the main source of $\text{Im}B_0$ and $\text{Im}C_0$ in the calculation by Chai and Riska.⁸

If the argument above is correct, it actually means that the microscopically calculated B_0 and C_0 , like those of Ref. 8, are inappropriate for use with the first-order optical potentials constructed on the basis of the free πN matrix t . They can only be used together with the optical potentials constructed without reference to the impulse approximation.

IV. APPLICATION OF THE $V^{(1)} + V^{(2)}$ MODEL

The model developed in Secs. II and III has been applied to the calculations of the total cross sections and elastic integral and differential cross sections of the posi-

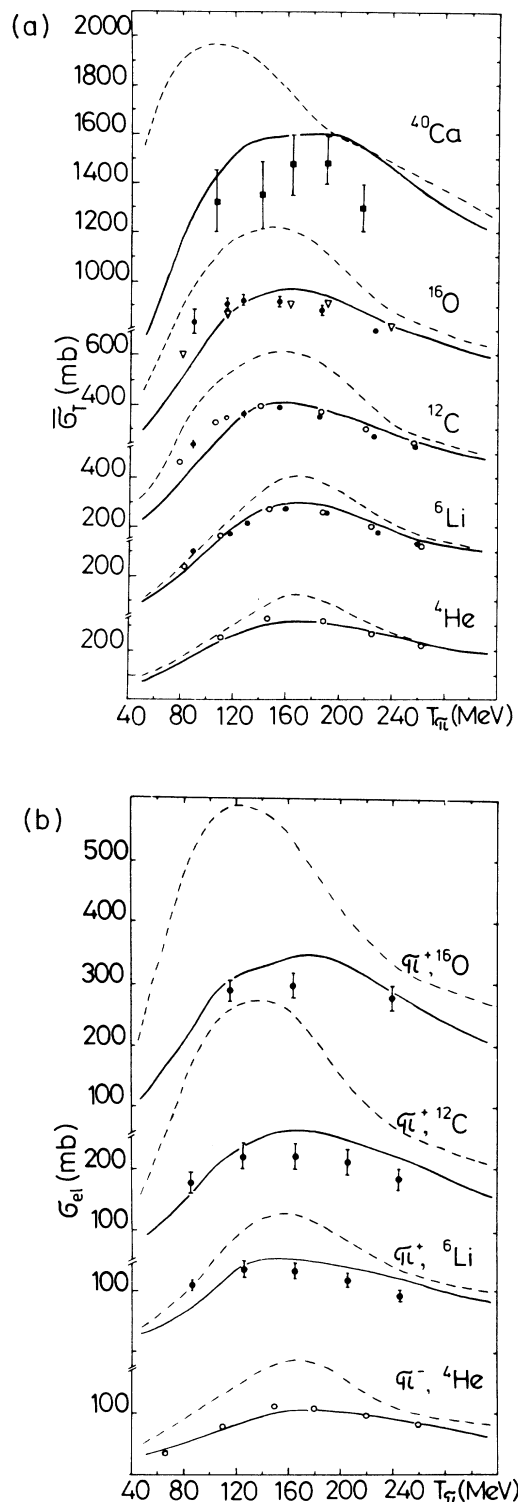


FIG. 3. Comparison with the data of calculated charge-averaged total cross sections ($\bar{\sigma}_T = \frac{1}{2}[\sigma_T(\pi^+) + \sigma_T(\pi^-)]$) and elastic cross sections (σ_{el}). The dashed (solid) curves represent the result for $V^{(1)}(V^{(1)} + V^{(2)})$. Data are taken as follows: (a) Ref. 32 (\circ : ^4He , ^6Li , ^{12}C), Ref. 33 (\bullet : ^6Li , ^{12}C , ^{16}O), Ref. 34 (∇ : ^{16}O), and Ref. 35 (\blacksquare : ^{40}Ca); (b) Ref. 36 (\circ : ^4He), Ref. 37 (\bullet : ^6Li , ^{12}C), and Ref. 38 (\bullet : ^{16}O).

tive and negative pions on ${}^4\text{He}$, ${}^6\text{Li}$, ${}^{16}\text{O}$, ${}^{28}\text{Si}$, and ${}^{40}\text{Ca}$. The corresponding results are shown in Figs. 4–8. We have consistently used the KMT formulation (Ref. 4, $S=1$) of the multiple-scattering theory.

In view of the standard good agreement between calcu-

lations and data, and for the economy of space, we mainly show the results for one charge of pions. The alternative-charge results are shown if some new feature can be demonstrated.

The total σ_T and elastic integral cross section σ_{el} are

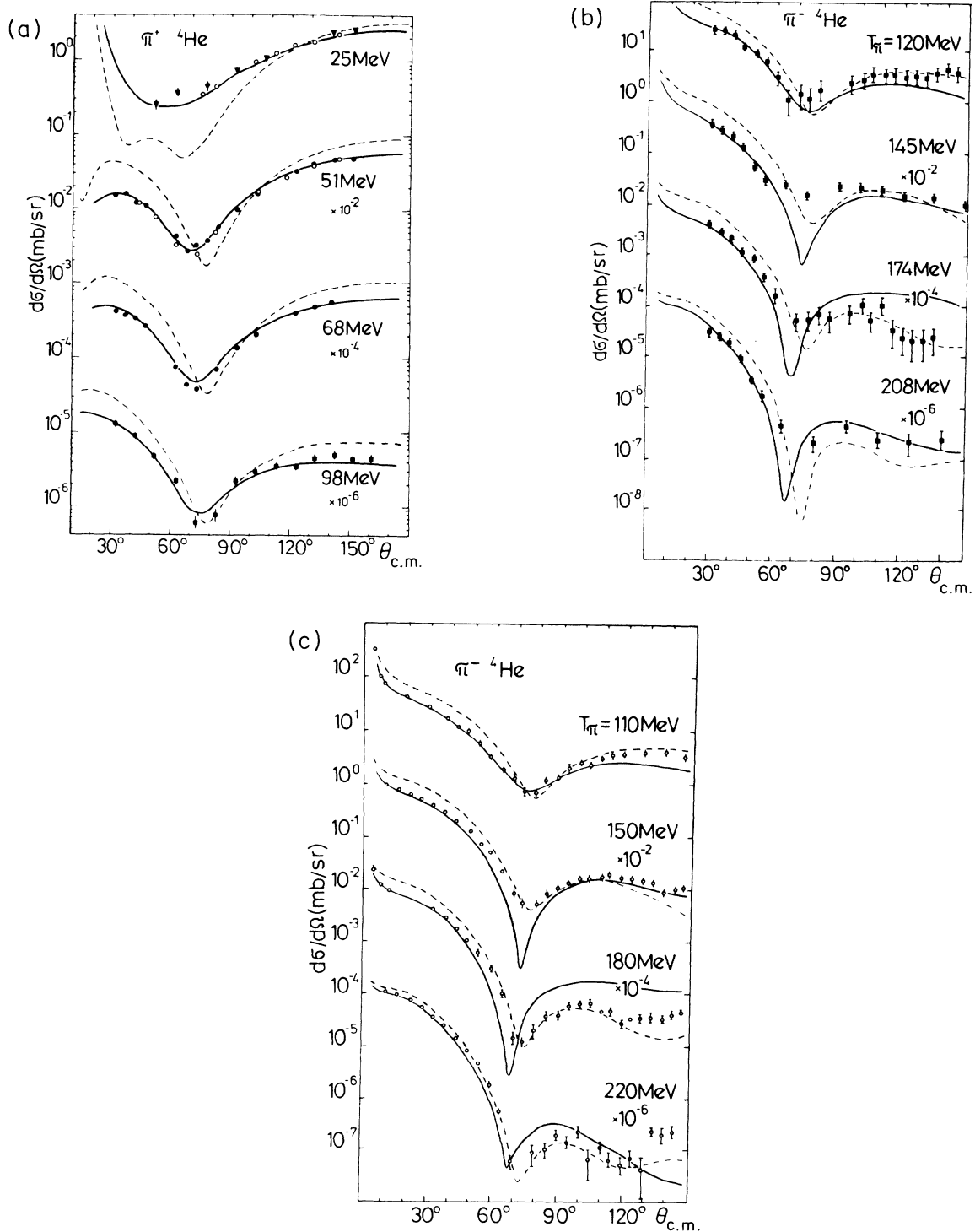


FIG. 4. The same as in Fig. 2 for π^- - ${}^4\text{He}$ scattering. For the data see Ref. 40 (\circ : 25 MeV), Ref. 41 (∇ : 24 MeV), Ref. 42 (51 and 68 MeV), Ref. 43 (98 MeV), Ref. 44 (120, 145, 174, and 208 MeV), and Ref. 36 (110, 150, 180, and 220 MeV).

shown in Fig. 3 for the cases where data are available. Inspection of the figure shows that a really important improvement of the theoretical description is achieved when including the ρ^2 -dependent term of the optical potential.

In some cases σ_T are measured individually for positive and negative pions. The corresponding calculated results (for the $V^{(1)} + V^{(2)}$ case) not shown here always correctly reproduce the observed difference of the π^+ and π^- data.

Going into more detailed discussion, one sees definite disagreement between theory and the data for the ^{12}C total cross section σ_T at lower energies. This is the only instance where we were unable to improve the theoretical description of σ_T by any smooth change of B_0 and C_0 not deteriorating the fit for the differential cross sections. On the other hand, it is gratifying to see that the calculations of σ_T and σ_{el} for the $A = 4, 6, 16,$ and 40 nuclei, both at low and resonance energies, which were performed without any free parameters, agree so nicely with the experimental data.

We now proceed to the discussion of the differential cross sections of the individual nuclei.

A. ^4He

The differential $\pi^-^4\text{He}$ cross sections calculated including (solid line) and omitting (dashed line) the $V^{(2)}$ term are compared in Fig. 4 with the data. One easily observes that the lower-energy ($T_p \leq 120$ MeV) theoretical results are in almost ideal agreement with the data over the entire measured range $10^\circ \leq \theta \leq 160^\circ$ if indeed the $V^{(2)}$ term is taken into account.

The resonance-energy $\pi^-^4\text{He}$ scattering has been experimentally studied by Binon *et al.*³⁶ and by Falomkin *et al.*⁴⁴ In our calculation we reproduce these data very well for $\theta \leq 60^\circ$, see Figs. 4(b) and 4(c). There are definite discrepancies between the theoretical and experimental results near the first minimum for $145 \leq T_\pi < 210$ MeV and at large scattering angles for the energies $T_\pi = 174$ and $T_\pi = 180$ MeV. For further discussion, see Sec. V.

B. ^6Li , ^{16}O , and ^{28}Si

The calculations for those three nuclei and the comparison of the theoretical results with the experimental data performed in Figs. 5–7 fully support our expectation of the universality of B_0 and C_0 and illustrate the high predictive power of the model developed in Secs. II and III.

The only serious discrepancy observed in this group of results concerns the 100 MeV π^+ scattering on ^6Li . The calculated differential cross section is much too low by a factor of about 1.5, even at small scattering angles. We do not understand this discrepancy. The total cross section σ_T at $T_\pi = 100$ MeV is obtained in agreement with the data, see Fig. 3. Note that Germond⁵² encountered similar difficulties with the 100 MeV differential cross section in his eikonal-type calculation, where the nucleon Fermi motion has been considered explicitly. Since Germond uses an αNN cluster model of ^6Li , several many-particle effects, which we just simulate by the ρ^2 term, are in his approach taken into account explicitly in terms of a

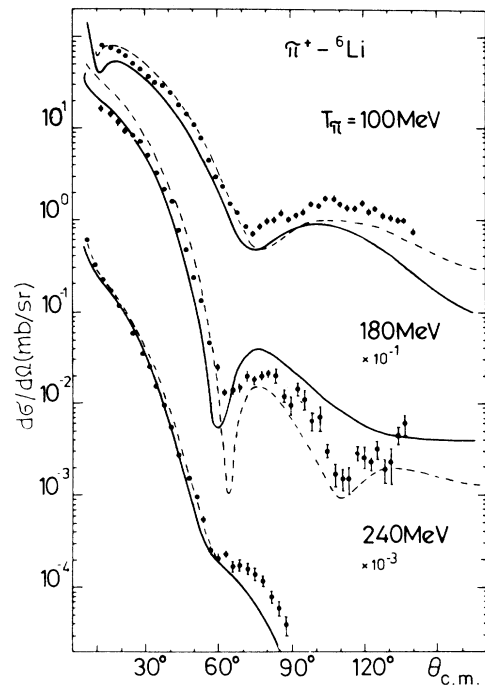


FIG. 5. The same as in Fig. 2 for the $\pi^+{}^6\text{Li}$ scattering. The data are from Ref. 45.

phenomenological $\pi^+{}^4\text{He}$ scattering amplitude.

The differential cross sections for the π^\pm scattering on ^{16}O and ^{28}Si at $80 \leq T_\pi \leq 225$ MeV shown in Figs. 6 and 7 as calculated in our $V^{(1)} + V^{(2)}$ model are surprisingly close to the data.

C. ^{40}Ca

In Figs. 8(a) and 8(b) we show our calculated $d\sigma/d\Omega$ for the $\pi^+{}^{40}\text{Ca}$ scattering at low and near-resonance energies, respectively. Their comparison with the data, which are also shown, demonstrates very clearly that the $V^{(2)}$ term again greatly improves the model used. It brings the theoretical $d\sigma/d\Omega$ into almost quantitative agreement with the experimental data, with the exception of the intermediate-angle ($50^\circ < \theta < 90^\circ$) interval for the 50, 60, and 80 MeV π^+ scattering. Let us discuss this case in more detail.

The Coulomb interaction in the ^{40}Ca nucleus is already strong enough and this may bring about a considerable difference of the π^+ and π^- differential cross sections. The experimental work reported in Ref. 48 for ^{40}Ca has shown that the difference is largest at $T_\pi = 60\text{--}80$ MeV and for the scattering angles $50^\circ \leq \theta \leq 80^\circ$: The π^- cross section is in this interval 3 times as large as that for the π^+ mesons.

According to the estimations we have performed, the strong dependence of the cross sections on the charge of incoming pions is probably connected with the difference of the proton and neutron distributions in ^{40}Ca . As a matter of fact, the neutron rms radius of ^{40}Ca as extracted from the 100 MeV α -particle- and 1 GeV proton-

scattering data seems to be by 10–20 % lower⁵³ as compared with the corresponding proton rms radius. In our calculations we have assumed that the proton and neutron distributions are identical.

To check further our $V^{(1)} + V^{(2)}$ model independently of the just mentioned difficulty, we decided to analyze also the mean differential cross sections,

$$\frac{d\bar{\sigma}}{d\Omega} = \frac{1}{2} \left[\frac{d\sigma}{d\Omega}(\pi^+) + \frac{d\sigma}{d\Omega}(\pi^-) \right],$$

which are indeed less sensitive to the Coulomb effects.

The mean differential cross sections at $T_\pi = 64.5$ and 80

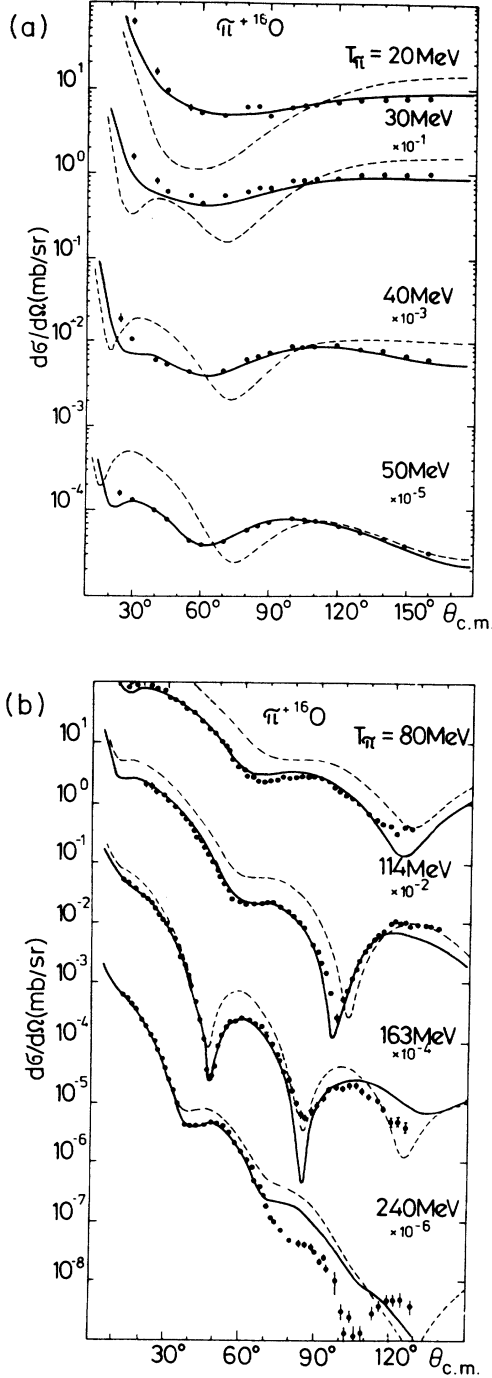


FIG. 6. The same as in Fig. 2 for the $\pi^{-16}\text{O}$ scattering. For data see Ref. 23 (20 MeV), Ref. 24 (30 and 50 MeV), Ref. 25 (40 MeV), and Ref. 46 ($T_\pi \geq 80$ MeV).

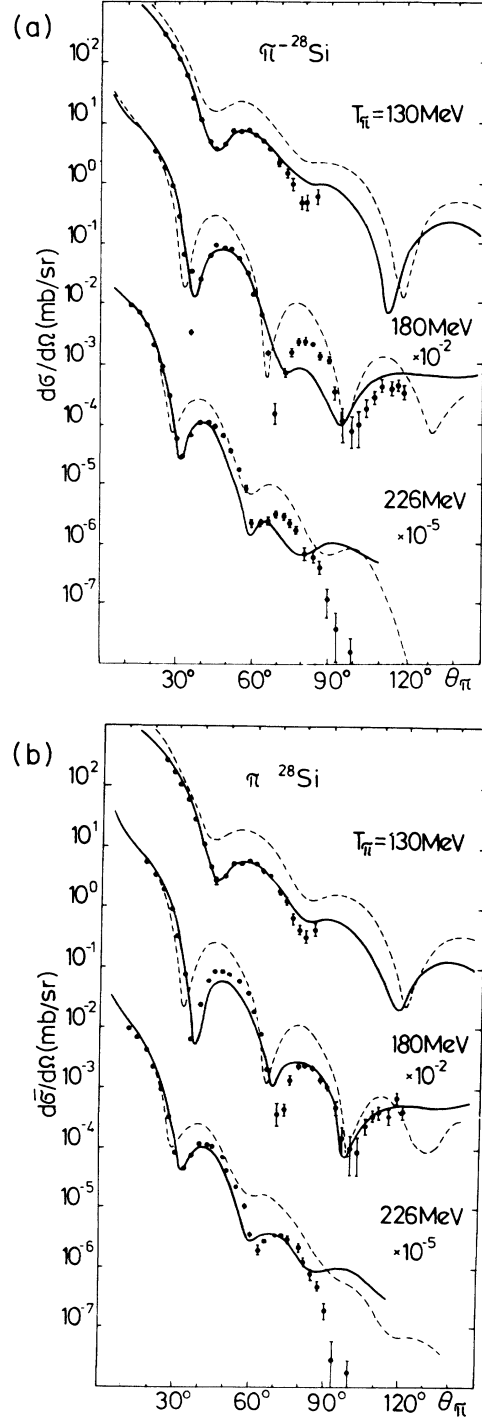


FIG. 7. Comparison of theoretical calculations with the experimental data (Ref. 47) for (a) π^+ scattering on ^{28}Si ; (b) charge-average $\pi^{-28}\text{Si}$ scattering ($d\bar{\sigma}/d\Omega = \frac{1}{2}[d\sigma(\pi^+)/d\Omega + d\sigma(\pi^-)/d\Omega]$); see also caption for Fig. 2.

MeV as shown in Fig. 8(c) are rather reasonably reproduced by our calculations. This strongly supports the argument above. Unfortunately, the data for π^- - ^{40}Ca scattering at $T_\pi=50$ MeV are not available and we cannot therefore extend our analysis to this case.

In the resonance-energy region the Coulomb effects are less important. In this situation we observe in Figs. 8(b) and 8(c), similarly to the cases of the lighter nuclei discussed above, a very close agreement of the results calculated with $V^{(1)} + V^{(2)}$ potential with data.

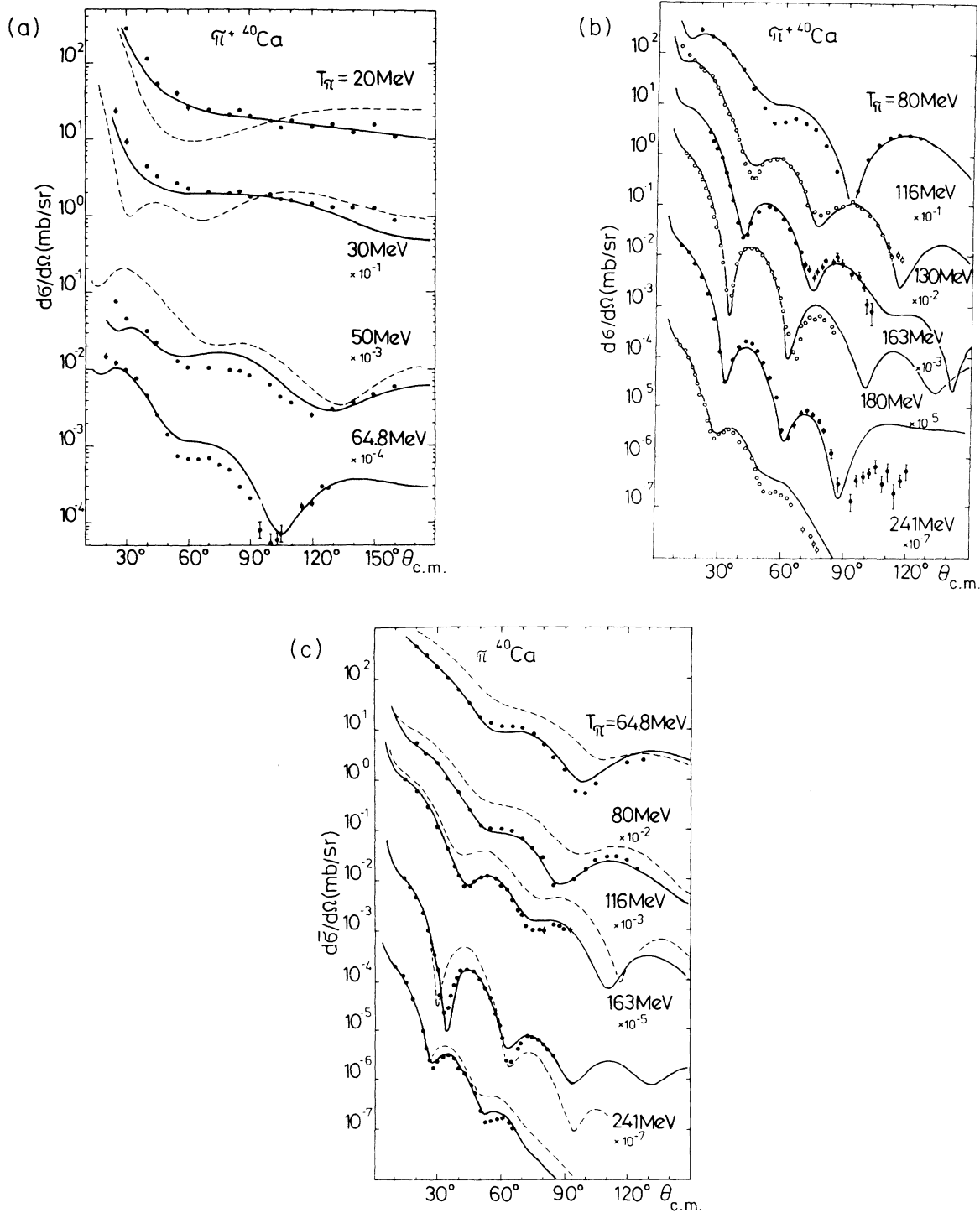


FIG. 8. The same as in Fig. 7 for π^- - ^{40}Ca scattering. For the data see Ref. 23 (20 MeV), Ref. 24 (30 and 50 MeV); Ref. 48 (64.8 MeV), Ref. 49 (80 MeV), Ref. 50 (130, 180, and 230 MeV), and Ref. 51 (116, 163, and 241 MeV).

V. DISCUSSION

Originally, we introduced the ρ^2 -dependent term with a very modest motivation: we just needed a better description of the pion distortion in our pion photoproduction work. To our pleasant surprise we have observed the striking A universality of the $V^{(2)}$ term derived through fitting the data for a single nucleus— ^{12}C . Nevertheless, in the preceding section we have seen that the universality of the model for $A \leq 40$, though spectacular, is indeed not complete: On one hand, we wish to stress that the potential $V^{(2)}$ constructed in Sec. III always guarantees a correct reproduction of the forward-angle data at all energies and for all nuclei studied, with the exception of the 100 MeV scattering off ^6Li . On the other hand, the agreement between calculations and data deteriorates sometimes at larger scattering angles and for the lightest nuclei.

If the general success of our model is due to the mutual cancellation of several correction terms omitted here, as we suppose, it is useful for the further analysis to enumerate the main approximations which we have used.

(i) The nucleon Fermi motion is taken into account only via effective nucleon momenta (2).

(ii) The ρ^2 term is actually a remnant of the pair correlation function,

$$C(\mathbf{r}', \mathbf{r}) = \frac{1}{A(A-1)} \sum_{i \neq k} \langle 0 | \delta(\mathbf{r}' - \mathbf{x}_k) \delta(\mathbf{r} - \mathbf{x}_i) | 0 \rangle \\ - \rho(\mathbf{r}') \rho(\mathbf{r}).$$

One actually follows the argument by Feshbach *et al.*:⁵⁴ Due to the repulsive nature of the NN potential at short distances, it is expected⁵⁴ that, for small internucleon distance,

$$C(\mathbf{r}', \mathbf{r}) \rightarrow -\rho^2(r) \text{ as } |\mathbf{r}' - \mathbf{r}| \rightarrow 0.$$

The long-range correlations are almost fully neglected by such a choice.

(iii) The energy shift (9) depends also on the angle between \mathbf{Q} and \mathbf{Q}' . In the calculation we have disregarded this dependence, taking

$$\Delta E = -\frac{\mu_2}{4M} \frac{A-2}{A} Q^2,$$

the choice appropriate for the forward scattering $\mathbf{Q} = \mathbf{Q}'$. [To avoid a misunderstanding, let us stress that the angular dependence of the energy shift (3) of the first-order potential $V^{(1)}$ is always taken into account in our calculations.]

(iv) The forward-scattering approximation was also used in Eq. (7): To obtain the $C_0(E)\mathbf{Q}\cdot\mathbf{Q}'/d^2$ term, we have assumed the model of independent nucleon pairs, which leads to the p -wave part of the ρ^2 term in the form $C_0(E)\mathbf{p}_2 \cdot \mathbf{p}'_2$, where

$$\mathbf{p}_2 = \frac{1 + m_\pi / Am_N}{1 + m_\pi / 2m_N} \mathbf{Q} - \frac{A-2}{2A} \frac{m_\pi}{m_\pi + 2m_N} (\mathbf{Q}' - \mathbf{Q}).$$

Now, assuming $m_\pi / Am_N \approx 0$ and $\mathbf{Q} \approx \mathbf{Q}'$, we arrive at $\mathbf{p}_2 \approx \mathbf{Q}/d$ and at Eq. (7).

It is indeed tempting to connect the difficulties mentioned above in Sec. IV in describing some cases of the backward-angle scattering on the lightest nuclei with the last two approximations. In the future work, which must indeed be directed towards a more accurate treatment of the nucleon Fermi motion, it will definitely be useful to avoid approximation (iii) and (iv).

From a purely empirical point of view, it seems that introducing a single additional energy-independent parameter in $V^{(2)}$ (take, e.g., $\exp[-2^2 q^2 / (A-1)]G(q)$ instead of the present $G(q)$) would allow us to get an almost perfect fit in all cases considered. Our numerical experience strongly supports this conjecture. Such a form does not change the presently obtained results at low energies and for the forward scattering at any energy. Simultaneously, the agreement reached here for σ_T and σ_{el} is not spoiled. Also, the results for the scattering on nuclei with $A > 12$ remain unaffected. The net effect of the correction factor is then the needed improvement of the differential cross sections at backward angles for the lightest nuclei. For the time being, we do not see, however, any possibility of a microscopic explanation for such an *ad hoc* factor.

Before concluding this section one should mention that the use of the KMT approach has proved to be decisive for the success of our model. Though no systematic search has been attempted, we must say that we have failed in looking for similar A -universal functions $B_0(E)$ and $C_0(E)$ within the Watson formulation of the multiple-scattering theory.

VI. CONCLUSIONS

We conclude the following.

(1) In the present work we have constructed an optical pion-nuclear potential in the momentum space. The potential contains two complex free parameters B_0 and C_0 in the ρ^2 -dependent term. This term was introduced phenomenologically and is intended to imitate the true pion absorption and the second-order optical potential effects. Numerical values of the parameters B_0 and C_0 were obtained from the π - ^{12}C scattering data and turned out to be independent of the atomic number of the target nucleus in the interval $4 \leq A \leq 40$ and also independent of the pion charge.

(2) Using the above potential model, we succeeded with one exception (100 MeV π^+ elastic scattering on ^6Li) to describe at a very good level of accuracy all available total and forward elastic differential cross section data for the ^4He , ^6Li , ^{16}O , ^{28}Si , and ^{40}Ca nuclei and $T_\pi \leq 250$ MeV. For the last three nuclei, very good results extend to the full observed angular range. This success shows that the A -dependence of the ρ^2 term has been correctly chosen as corresponding to the dominance of the two-body effects among other many-particle contributions left out in the first-order potential.

(3) It seems to be generally accepted that one cannot simultaneously reproduce the observed total and differential cross sections using only a first-order pion-nucleus optical potential. Earlier, it was shown² that the assumption of pion propagation modified by the medium corrections can adequately explain the total and elastic

TABLE II. Parameters of the symmetrized Fermi density distribution, taken from Ref. 21.

Nucleus	⁴ He	⁶ Li	¹² C	¹⁶ O	²⁸ Si	⁴⁰ Ca
b (fm)	0.300	0.566	0.393	0.404	0.477	0.493
c (fm)	1.251	1.342	2.275	2.624	3.134	3.593

scattering data provided a “spreading potential” fitted to the total and forward-elastic cross sections is introduced. From the results presented here it is seen that the phenomenological ρ^2 term serves the purpose similarly well since it introduces the needed corrections which go beyond the impulse approximation inherent in the potential $V^{(1)}$.

(4) The parameters B_0 and C_0 are energy dependent and strongly enhanced near $E_\pi=170-180$ MeV. This type of the energy dependence indeed shows the important role of the resonance mechanism of the pion absorption which proceeds via creation of a Δ isobar.

(5) At low pion energies the parameters B_0 and C_0 are close to the value obtained from the mesoatomic data via the optical potential of Stricker, McManus, and Carr.¹⁹

(6) The optical potential constructed in the present work can be successfully used, not only in the forthcoming analysis of the elastic scattering data, but also for the theoretical work on inelastic pion scattering and pion photoproduction in the distorted-wave impulse approximation approach in the momentum space, which, by now, has become most popular. Simultaneously, the existence of the universal coefficients B_0 and C_0 as obtained in this work should stimulate further microscopic studies of the two-body mechanisms of the pion-nuclear interactions, particularly the true pion absorption.

ACKNOWLEDGMENTS

We express our thanks to V. V. Burov and V. K. Lukyanov for supplying us with their results on the symmetrized Fermi density. We wish to acknowledge gratefully numerous discussions with and comments by R. A. Eramzhyan, M. K. Khankasayev, and M. G. Sapozhnikov. One of us (M.G.) thankfully acknowledges inspiring conversations with F. Lenz and M. Locher and their hospitality at SIN.

$$G^{\text{SF}}(r) = \frac{(2\pi\rho_0 b)^2}{q \sinh(\pi b q)} \left\{ \cos(qc) \left[1 - \pi b q \coth(\pi b q) - \frac{c}{b} \coth\left(\frac{c}{b}\right) \right] + \sin(qc) \left[\pi \coth(\pi b q) \coth\left(\frac{c}{b}\right) - q c \right] \right\}. \quad (\text{A5})$$

APPENDIX

In the construction of the potentials $V^{(1)}$ [Eq. (4)] and $V^{(2)}$ [Eq. (7)], we have used the symmetrized Fermi density $\rho_{\text{SF}}(r)$. It has the form

$$\rho_{\text{SF}}(r) = \rho_0 \frac{\sinh(c/b)}{\cosh(c/b) + \cosh(r/b)}, \quad (\text{A1})$$

$$\rho_0 = \frac{3}{4\pi c^3} \left[1 + \left(\frac{\pi b}{c} \right)^2 \right]^{-1},$$

and is known to reproduce well the nuclear charge form factors for $4 \leq A \leq 40$ in a broad interval of the transferred momenta, $0 \leq q \leq 4$ fm⁻¹. The parameters b and c of Eq. (A1) were obtained in Ref. 21 from an analysis of the electron-scattering data and are listed in Table II.

The form factor corresponding to (A1) is²¹

$$F_0^{\text{SF}}(q) = \rho_0 \frac{4\pi^2 b c}{q \sinh(\pi b q)} \left[\frac{\pi b}{c} \coth(\pi b q) \sin(qc) - \cos(qc) \right]. \quad (\text{A2})$$

To derive the Fourier transform $G(q)$ of the density squared defined in Eq. (8), we use the identity

$$\int_0^\infty r \rho_{\text{SF}}^2(r) \sin(qr) dr = \rho_0^2 \sinh^2(c/b) \frac{\partial^2}{\partial q \partial a} I(a, q), \quad (\text{A3})$$

where $a = \cosh(c/b)$, and

$$I(a, q) = \int_0^\infty \frac{\cos(qr)}{a + \cosh(r/b)} dr$$

$$= \frac{\pi b}{(a^2 - 1)^{1/2}} \frac{\sin[bq \arccos(a)]}{\sinh(\pi b q)}. \quad (\text{A4})$$

Combining Eqs. (A3) and (A4), we find

¹L. S. Kisslinger and W. L. Wang, Phys. Rev. Lett. **30**, 1071 (1973); Ann. Phys. (N.Y.) **99**, 374 (1976); W. Weise, Nucl. Phys. **A278**, 402 (1977).

²Y. Horikawa, M. Thies, and F. Lenz, Nucl. Phys. **A345**, 386 (1980); F. Lenz, M. Thies, and Y. Horikawa, Ann. Phys. (N.Y.) **140**, 266 (1982); M. Hirata, F. Lenz, and M. Thies, Phys. Rev. C **28**, 785 (1983).

³M. Goldberger and K. M. Watson, *Collision Theory* (Wiley,

New York, 1964).

⁴A. K. Kerman, H. McManus, and R. M. Thaler, Ann. Phys. (N.Y.) **8**, 551 (1959).

⁵R. H. Landau and A. W. Thomas, Nucl. Phys. **A302**, 461 (1978); J. P. Maillet, J. P. Dedonder, and C. Schmit, *ibid.* **A271**, 253 (1976).

⁶L. C. Liu and C. M. Shakin, Prog. Part. Nucl. Phys. **5**, 207 (1981).

- ⁷M. Gmitro, J. Kvasil, and R. Mach, *Phys. Rev. C* **31**, 1349 (1985).
- ⁸J. Chai and D. O. Riska, *Nucl. Phys.* **A329**, 429 (1979).
- ⁹E. Oset, W. Weise, and R. Brockman, *Phys. Lett.* **82B**, 344 (1979).
- ¹⁰L. Tiator and L. E. Wright, *Phys. Rev. C* **30**, 989 (1984); L. Tiator, *Phys. Lett.* **125B**, 367 (1983).
- ¹¹R. A. Eramzhyan, M. Gmitro, S. S. Kamalov, and R. Mach, *J. Phys. G* **9**, 605 (1983).
- ¹²M. Ericson and T. E. O. Ericson, *Ann. Phys. (N.Y.)* **36**, 323 (1966).
- ¹³R. Mach, *Czech. J. Phys.* **33**, 616 (1983).
- ¹⁴M. I. Haftel and F. Tabakin, *Nucl. Phys.* **A158**, 1 (1970).
- ¹⁵C. M. Vincent and S. C. Phatak, *Phys. Rev. C* **10**, 391 (1974).
- ¹⁶R. A. Eramzhyan, M. Gmitro, T. D. Kaipov, S. S. Kamalov, and R. Mach, *Nucl. Phys.* **A429**, 403 (1984).
- ¹⁷M. Gmitro, S. S. Kamalov, R. Mach, and M. G. Sapozhnikov, *Yad. Fiz.* **40**, 107 (1984) [*Sov. J. Nucl. Phys.* **40**, 68 (1984)].
- ¹⁸J. M. Eisenberg and D. S. Koltun, *Theory of Meson Interactions With Nuclei* (Wiley, New York, 1980).
- ¹⁹K. Stricker, H. McManus, and J. Carr, *Phys. Rev. C* **19**, 929 (1979).
- ²⁰P. C. Tandy and R. M. Thaler, *Phys. Rev. C* **22**, 2321 (1980).
- ²¹V. V. Burov and V. K. Lukyanov, Joint Institute of Nuclear Research, Dubna, Report, P4-11098, 1977.
- ²²D. R. Gill, K. L. Erdman, E. W. Blackmore, W. Gyles, B. M. Barnett, C. Oram, R. R. Johnson, T. G. Masterson, and N. Grion, *Phys. Rev. C* **26**, 1306 (1982).
- ²³F. E. Obenshaim *et al.*, *Phys. Rev. C* **27**, 2753 (1983).
- ²⁴B. M. Preedom *et al.*, *Phys. Rev. C* **23**, 1134 (1981).
- ²⁵F. E. Bertrand *et al.*, *Phys. Rev. C* **20**, 1884 (1979).
- ²⁶R. R. Johnson, T. G. Masterson, K. L. Erdman, A. W. Thomas, and R. H. Landau, *Nucl. Phys.* **A296**, 444 (1978).
- ²⁷J. F. Amann, P. D. Barnes, K. R. Grass, S. A. Dytman, R. A. Einstein, J. D. Sherman, and W. R. Wharton, *Phys. Rev. C* **23**, 1635 (1981).
- ²⁸M. Blecher *et al.*, *Phys. Rev. C* **28**, 2033 (1983).
- ²⁹L. E. Antonuk *et al.*, *Nucl. Phys.* **A420**, 435 (1984).
- ³⁰J. Piffaretti, R. Corfu, J.-P. Egger, R. Gretillat, C. Lunke, E. Schwarz, C. Perrin, and B. M. Preedom, *Phys. Lett.* **71B**, 324 (1977).
- ³¹F. Binon, P. Duteil, J. P. Garron, J. Gorres, L. Hugon, J. P. Peigneux, C. Schmit, M. Spighel, and J. P. Stroot, *Nucl. Phys.* **B17**, 168 (1970).
- ³²C. Wilkin, C. R. Cox, J. J. Domingo, K. Gabathuler, E. Pedroni, J. Rohlin, P. Schwaller, and N. W. Tanner, *Nucl. Phys.* **B62**, 61 (1973).
- ³³A. S. Clough *et al.*, *Nucl. Phys.* **B76**, 15 (1974).
- ³⁴R. Jaeckle, H. Pilkuhn, and H. G. Schlaile, *Phys. Lett.* **B76**, 177 (1978).
- ³⁵R. H. Jeppesen *et al.*, *Phys. Rev. C* **27**, 697 (1983).
- ³⁶F. Binon, P. Duteil, M. Guanere, L. Hugon, J. Jansen, J.-P. Lagnaux, H. Palevsky, J.-P. Peigneux, M. Spighel, and J.-P. Stroot, *Nucl. Phys.* **A298**, 499 (1978).
- ³⁷D. Ashery, I. Navon, G. Azuelos, H. K. Walter, H. J. Pfeiffer, and F. W. Schlepütz, *Phys. Rev. C* **23**, 2173 (1981).
- ³⁸S. Ciulli, H. Pilkuhn, and H. G. Schlaile, *Z. Phys. A* **302**, 42 (1981).
- ³⁹P. C. Tandy, E. F. Redish, and D. Bollé, *Phys. Rev. C* **16**, 1924 (1977).
- ⁴⁰G. Fournier, A. Gerard, J. Miller, J. Picard, B. Saghai, P. Vernin, P. Y. Bertin, B. Coupat, E. W. A. Lingeman, and K. K. Seth, *Nucl. Phys.* **A426**, 542 (1984).
- ⁴¹M. E. Nordberg and K. F. Kinsey, *Phys. Lett.* **20**, 692 (1966).
- ⁴²K. M. Crowe, A. Fainberg, J. Miller, and A. S. L. Parsons, *Phys. Rev.* **180**, 1349 (1969).
- ⁴³Yu. A. Shcherbakov *et al.*, *Nuovo Cimento* **31A**, 249 (1976).
- ⁴⁴I. V. Falomkin *et al.*, *Nuovo Cimento* **43A**, 219 (1978).
- ⁴⁵L. E. Antonuk *et al.*, *Nucl. Phys.* **A451**, 741 (1986).
- ⁴⁶J. P. Albanèse, J. Arvieux, J. Bolger, E. Boschitz, C. H. Q. Ingram, J. Jensen, and J. Zichy, *Nucl. Phys.* **A350**, 301 (1980).
- ⁴⁷B. M. Preedom, R. Corfu, J. P. Egger, P. Gretillat, C. Lunke, J. Piffaretti, E. Schwarz, J. Jansen, and C. Perrin, *Nucl. Phys.* **A326**, 385 (1979).
- ⁴⁸S. E. Dam *et al.*, *Phys. Rev. C* **25**, 2574 (1982).
- ⁴⁹M. J. Leitch *et al.*, *Phys. Rev. C* **29**, 561 (1984).
- ⁵⁰P. Gretillat, J.-P. Egger, J. F. Germond, C. Lunke, E. Schwarz, C. Perrin, and B. M. Preedom, *Nucl. Phys.* **A364**, 270 (1981).
- ⁵¹O. Ingram, E. Boschitz, L. Pflug, J. Zichy, J. P. Albanèse, and J. Arvieux, *Phys. Lett.* **76B**, 173 (1978).
- ⁵²J. F. Germond, *J. Phys. G* **12**, 609 (1986).
- ⁵³K. G. Boyer *et al.*, *Phys. Rev. C* **29**, 182 (1984).
- ⁵⁴H. Feschbach, A. Gal, and J. Hüfner, *Ann. Phys. (N.Y.)* **66**, 20 (1971).
- ⁵⁵J. T. Londergan, K. M. McVoy, and E. J. Moniz, *Ann. Phys. (N.Y.)* **78**, 299 (1973).
- ⁵⁶E. R. Siciliano, M. D. Cooper, M. B. Johnson, and M. J. Leitch, *Phys. Rev. C* **34**, 267 (1986); S. J. Greene, C. J. Harvey, P. A. Seidl, R. Gilman, E. R. Siciliano, and M. B. Johnson, *ibid.* **30**, 2003 (1984).